

Proteins immobilization onto poly(acrylic acid) functional macroporous PolyHIPE via surface initiated ARGET ATRP from multi-tasking amino-polyHIPE precursor.

Fabrice Audouin<sup>1</sup>, Ruth Larragy<sup>2</sup>, Mary Fox<sup>2</sup>, Brendan O'Connor<sup>2</sup>, Andreas Heise<sup>1\*</sup>

<sup>1</sup>School of Chemical Sciences, Dublin City University, Glasnevin, Dublin 9, Ireland.

<sup>2</sup>Irish Separation Science Cluster, National Centre for Sensor Research, Dublin City University, Glasnevin, Dublin 9, Ireland

\* email: [andreas.heise@dcu.ie](mailto:andreas.heise@dcu.ie). Tel: 00353-1-7006709. Fax: 00353-1-7005503.

**Abstract:****Introduction**

The immobilization of biomolecules on solid support is of great interest for biosensors and bioseparation applications.<sup>1</sup> Active biomolecules, such as enzymes and antibodies, are generally employed as recognition elements in these applications due to their highly specific substrate affinity. The main considerations for employing bound biomolecules are their stability, activity and concentration. Covalent binding to a substrate can in many cases enhance the biomolecule stability and by choice of an appropriate chemistry even improve its bioactivity by reducing steric constraints and denaturation induced by the solid substrate.<sup>1,2</sup> Polymer brushes are particularly suited for covalent immobilization of biomolecules because they possess a well-defined structure, excellent mechanical stability and dense functional groups.<sup>3,4,5,6,7,8,9,10</sup> Moreover, the number of binding sites for biomolecules can be controlled by the polymer chain length. While this concept is particularly successful for planar and inorganic substrates, the decoration of three-dimensional macroporous polymeric substrates with polymer brushes provides a significantly bigger challenge. Macroporous polymeric substrates combine high surface area with excellent flow and mass transport properties and are thus ideally suited for a variety of applications including column filtration/separation, supported organic chemistry and as media for tissue engineering and 3D cell culture.<sup>11</sup> A material that has received increasing attention in that respect is prepared from concentrated high internal phase emulsions (HIPE) containing more than 74% internal phase volume.<sup>12,13,14,15</sup> If the continuous phase contains one or more monomeric species and polymerization is initiated, highly porous materials referred to as polyHIPEs are produced once the dispersed phase droplets are removed. Initially developed by Unilever<sup>16</sup>, polyHIPE preparation traditionally involves the formation of a stable concentrated water-in-oil emulsion using hydrophobic monomers as part of the continuous phase and an aqueous phase as the dispersed phase.<sup>17,18</sup> Introducing a homogeneous, highly dense layer of functional groups available for bioconjugation to the macroporous surface is essential to advance polyHIPE applications in areas biosensing and biosepara-

tion. Currently only few publications discuss the modification of polyHIPE surfaces with polymer brushes. In initial reports we as well as Maillard disclosed the incorporation of a polymerizable initiator (inimer) for atom transfer radical polymerization (ATRP) into a pHIPE and the subsequent surface grafting reaction by ATRP of methyl methacrylate (MMA).<sup>19,20</sup> We latter extended this approach to the grafting of glycidyl methacrylate (GMA) resulting in highly functional polyHIPE, which could be used as a reactive platform for example for “click” chemistry to efficiently decorate the polyHIPE surface.<sup>21</sup> While this approach resulted in a very homogeneous polyacrylate coating of the pore surfaces, the complete removal of the ATRP copper catalyst by washing was very tedious and often incomplete resulting in green monoliths. Moreover, the use of inimers in the polyHIPE synthesis is very restrictive, as they have to be specifically synthesized for the polymerization technique employed. We are thus interested in developing a universal polyHIPE platform that can easily be used to grow polymer brushes using different polymerization techniques. For this we recently disclosed a new class of primary amine functional macroporous polyHIPEs (polyHIPE-NH<sub>2</sub>) by the incorporation of a polymerizable monomer with a pendant amino group into a styrene/divinylbenzene HIPE formulation. In the first instance the surface amino groups were successfully used for the ring-opening polymerization of benzyl-L-glutamate (BLG) N-carboxyanhydride (NCA) and benzyloxycarbonyl-L-lysine (Lys(Z)) NCA resulting in a dense coating of polypeptides on the macroporous polyHIPE surface. After in-situ deprotection the polypeptide functionalized polyHIPEs were rendered pH responsive and the functional groups were available for further bioconjugation.<sup>22</sup> Despite this successful polypeptide grafting, the use of a controlled radical technique is much more desirable as it offers the possibility to draw on a large variety of commercially available functional monomers. In this work, we thus show that the universal primary amine functional polyHIPE can readily be converted into ATRP initiator functional polyHIPE. In order to overcome the drawback caused by high copper concentrations we employed activator regeneration by electron transfer (ARGET) ATRP for the synthesis of poly(acrylic acid) grafted polyHIPE.<sup>23,24</sup> Bioconjugation was studied by the covalent attachment of

fluorescent proteins, such as enhanced green fluorescent protein (eGFP) and coral derived red fluorescent protein (DsRed) to the poly(acrylic acid) coated polyHIPE. **eGFP is a mutated version of a green fluorescent protein first isolated from the jellyfish *Aequorea victoria* (Shimomura, Johnson and Saiga, 1962) which has enhanced fluorescence compared to the wildtype protein.**

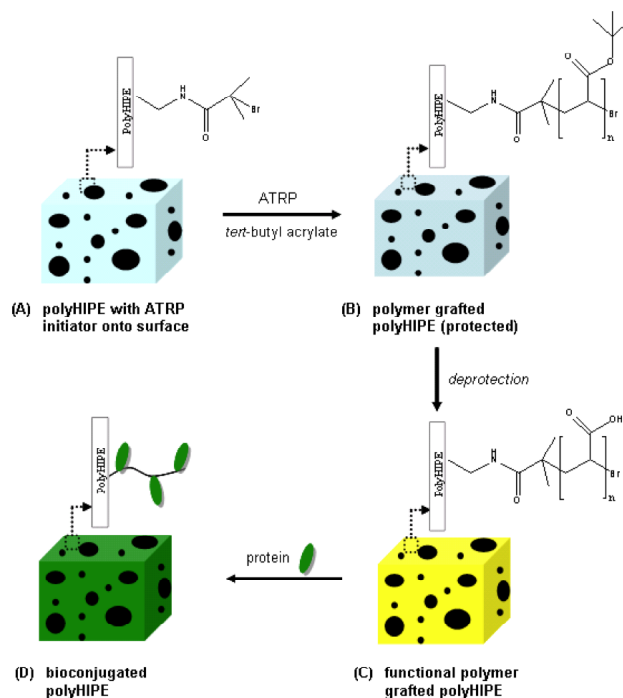


Figure 1. Synthetic pathway to poly(acrylic acid) grafted polyHIPE and subsequent bioconjugation.

## Experimental Part

**Materials.** 4-vinylbenzylphthalimide was synthesized following a literature procedure.<sup>25</sup> Methyl methacrylate (MMA, Aldrich 99 %) was distilled from calcium hydride prior to use. *Tert*-butyl acrylate (*t*BA, Aldrich 98%) was passed through a column of basic alumina to remove inhibitor. Anhydrous tetrahydrofuran (THF) was used directly from the bottle under an inert and dry atmosphere. All others chemicals were purchased from Sigma-Aldrich and used as received unless otherwise noted.

**Methods.**  $^1\text{H}$  NMR analyses were performed in  $\text{CDCl}_3$  solution at  $25^\circ\text{C}$  using a Bruker Avance 400 (400 MHz) spectrometer. Molecular weights of polymer were characterized by gel permeation chromatography performed on an Agilent 1200 series equipped with two PL Gel 5  $\mu\text{m}$  Mixed-C  $300 \times 7.5$   $\text{mm}^2$  columns at  $40^\circ\text{C}$  and a DRI detector. Tetrahydrofuran was used as an eluent at a flow rate of  $1\text{ mL min}^{-1}$ . Molecular weights were calculated based on poly(methyl methacrylate) (PMMA) standards. Thermogravimetric analyses (TGA) were performed on a TGA Q50 from TA Instrument using a temperature ramp from 20 to  $800^\circ\text{C}$  at  $20^\circ\text{C min}^{-1}$  (the weight loss is denoted W %) under nitrogen atmosphere. Scanning electron microscopy (SEM) was performed on a Hitachi S3400 with samples previously coated with gold using vapour deposition before analysis. Fourier Transform InfraRed (FTIR) spectroscopy was done in solid state on a Perkin Elmer Spectrum 100. Wettability tests of polyHIPEs was performed using a FTÅ200 dynamic contact angle analyser and on dried samples. An inverted fluorescence microscope (IX81, Olympus Co., Japan) equipped with an EMCCD camera (DV887-BI, Andor Technology, UK) and an MT20 fluorescence illumination unit fitted with a 150 W xenon lamp was used in combination with a FITC filter set to image the green fluorescence of the eGFP immobilized onto the polyHIPE-g-PAA and was used with a CYS filter set to image the red fluorescence of the DsRed immobilized onto the polyHIPE-g-PAA. The fluorescent images were acquired using the Cell^R software (Olympus Soft Imaging Solutions, GmbH, Germany), and all fluorescent images were acquired using the same set of parameters.

*Synthesis of polyHIPE-NH<sub>2</sub>.* 1.7 g (0.0163 mol) of styrene, 0.7 g (0.0053 mol) of divinylbenzene, 0.4 g (0.0015 mol) of 4-vinylbenzylphtalimide and 0.8 g of Span 80 surfactant were placed in a reactor and the mixture stirred using an overhead stirrer at 300 rpm. The aqueous solution was prepared by dissolving 0.3 g of potassium peroxodisulfate ( $\text{K}_2\text{S}_2\text{O}_8$ ) in 25.5 ml of deionised water and 17 ml of the prepared aqueous solution was used as the internal phase. It was added dropwise to the monomer solution under constant stirring. Once all aqueous phase was added, stirring was continued for a further 20 minutes to produce a uniform emulsion. Afterwards, the emulsion was transferred to a glass mold

and heated at 60°C for 24 hours. The resulting monoliths were washed with THF (3\*250ml), then acetone (2\*250ml) before drying in vacuo at 40°C overnight. The phthalimide group was removed by vigorously stirring the polyHIPE (500 mg) in a solution of 150 ml ethanol containing *tert*-butylcatechol (60 mg). Then, 5 ml of hydrazine monohydrate was added and the solution was heated under reflux during 24 hours. Afterwards the polyHIPE was washed three times with 150 ml of ethanol before drying under vacuum. The final porosity of the polyHIPE measured by intrusion of mercury analysis was 83 %. (our ref)

*Immobilization of ATRP initiator on polyHIPE-NH<sub>2</sub>.* The available amino groups on the surface were converted into ATRP initiators by immersing the polyHIPE-NH<sub>2</sub> (700 mg) under nitrogen atmosphere into 100 ml of anhydrous THF and triethylamine (0.1 ml, 0.71 mmol). Then, the solution was cooled down at 0°C before the dropwise addition of  $\alpha$ -bromoisobutyryl bromide (0.15 g, 0.65 mmol). After 1 hour at 0°C, the reaction was allowed to stand at room temperature overnight. Thereafter, the monolith was washed with THF (2  $\times$  100 ml) and acetone (2  $\times$  100 ml) to remove residual reactant and by-product. The polyHIPE was finally dried in a vacuum oven.

*Grafting of methyl methacrylate and tert-butyl acrylate from ATRP initiator functionalized polyHIPE* (representative example for PHIPE-g-PMMA<sub>2</sub>). The initiator modified polyHIPE (70 mg) was immersed into a Schlenk tube containing anisole (4.0 g), MMA (4.68 g, 0.0467 mol.), Cu(II)Br<sub>2</sub> (1.4 mg, 0.0062 mmol.), PMDETA ( mg, 0.062 mmol.) and EBiB ( mg, 0.062 mmol.). The Schlenk tube was sealed with a rubber septum and the solution degassed with nitrogen for 20 minutes. Then, tin(II) 2-ethylhexanoate (25 mg, 0.062 mmol) in anisole (0.975 g) was added to the solution and the Schlenk tube was placed in a thermostated oil bath at 30°C. When the polymerization time was reached, the reaction solution was exposed to air. The grafted polyHIPE was transferred to an Erlenmeyer flask and thoroughly washed twice in 50 ml THF, two times with 50 ml acetone and finally dried in a vacuum oven. In case a sacrificial initiator was used, the free polymer was diluted with THF and passed

through a neutral alumina column before to be precipitated in cold methanol, and thereafter dried in a vacuum oven. For ARGET ATRP of *t*BA from the polyHIPE surface, the general procedure was similar and the experimental conditions summarized in table 1 were used.

Table1. Experimental conditions for the MMA and *t*BA ARGET ATRP from the polyHIPE-Br surface.

Entry	PHIPE-Br (mg)	EBiB (mg)	CuBr <sub>2</sub> (mg)	Ligand (mg)	Monomer (g)	Anisole (g)	Tin(II) (mg)	Temp. (°C)
PHIPE-g-PMMA1	70	-	1.4	10.8	4.68	4.975	25	30
PHIPE-g-PMMA2	70	12.2	1.4	10.8	4.68	4.975	25	30
PHIPE-g-PtBA1	70	-	0.7	5.4	4.375	4.975	12.5	60
PHIPE-g-PtBA2	70	6.1	0.7	5.4	4.375	4.975	12.5	60
PHIPE-g-PtBA3	70	-	0.7	9	4.375	4.975	12.5	60
PHIPE-g-PtBA4	70	6.1	0.7	9	4.375	4.975	12.5	60
PHIPE-g-PtBA5	70	6.1	0.7	9	4.375	4.975	12.5	60
PHIPE-g-PtBA6	70	12.2	1.4	18	4.375	4.975	25	60

*Conversion of PHIPE-g-PtBA into PHIPE-g-PAA.* The polyHIPE substrate (around 100 mg) covered with PtBA were placed into a flask, which contained a mixture of 12 mL of 1,4-dioxane and 4 mL of concentrated HCl (37%). The flask was connected to a condenser, and the solution was heated to reflux

for 24 hours. Then, the samples were removed and thoroughly washed 2 times with 20 ml of 1,4-dioxane and 2 times with 20 ml of acetone and dried under vacuo.

*Expression and purification of recombinant eGFP and DsRed proteins.* The eGFP and DsRed proteins were expressed and purified in an identical manner. A plasmid vector encoding the N-terminal histidine-tagged protein was transformed into the *E. coli* strain KRX. The bacteria was cultured in 100 ml of TB broth, overnight at 30°C. Protein expression was induced with 50 µg/ml IPTG. The cells were harvested and disrupted by high pressure using a Constant Systems Cell disrupter. The protein was purified over Ni Sepharose (GE Healthcare) with elution using 250 mM imidazole. The eluted protein containing fractions were buffer exchanged using Vivaspin centrifugal concentrators (Sartorius), with a molecular weight cut off of 10 kDa.

*Fluorescent protein (eGFP and DsRed) immobilization onto the polyHIPE-g-PAA.* The experimental conditions for the eGFP and DsRed immobilization onto polyHIPE-g-PAA are given in Table . For the eGFP conjugation, 2.5 mg of polyHIPE-g-PAA6 was mixed with 0.5 mg of N-hydroxysulfosuccinimide sodium salt (sulfo-NHS) in 0.5 ml of phosphate buffered saline (PBS, pH = 7.4). Then, a solution of 1 mg of 1-ethyl-3-(3-dimethylaminopropyl) carbodiimide hydrochloride (EDC) in 1 ml PBS was added and mixed together for 30 min. Afterwards, 1.6 ml of eGFP in PBS (1.5 mg of protein per 1 ml of PBS) and 10 µl 4-(dimethylamino)pyridine (DMAP) in PBS solution (1 mg of DMAP per 1 ml PBS) were added and the solution stirred for 2 days at room temperature. The material was subsequently washed extensively with the same buffer solution to remove any unbound protein, then with DI water and dried under vacuo at room temperature for 24 hours. Similar procedure was used for DsRed immobilization.

Table 2 Experimental conditions for the eGFP and DsRed immobilization onto polyHIPE-g-PAA (PHIPE-g-PAA6 used in all experiments)



Entry	pHIPE-g-PAA6 (mg)	protein buffer (ml)	Sulfo-NHS (mg)	EDC (mg)	DMAP (mg)	Buffer (ml)
PeGFP1	2.5	1.6 <sup>a[1.5]</sup>	0.5	1	0.01	1.5 <sup>a</sup>
PeGFP2	2.5	1.3 <sup>b[1.9]</sup>	0.5	1	-	1.8 <sup>b</sup>
PDsRed1	2.5	1.2 <sup>a[2.0]</sup>	0.5	1	0.01	2 <sup>a</sup>
PDsRed2	2.5	0.8 <sup>[2.9]</sup>	0.5	1	-	2.2 <sup>c</sup>

(a) PBS buffer solution pH = 7.4. (b) Sodium carbonate buffer solution pH = 8.6 (c) Sodium carbonate buffer solution pH = 9.7 [x] protein concentration in mg/ml.

## Results and Discussion

### *Grafting of polymer from ATRP functional polyHIPEs*

Amine functional polyHIPE was obtained as previously described<sup>REF</sup> and reacted with  $\alpha$ -bromoisobutyryl bromide (BIBB) to form a uniform ATRP initiator layer on the monolith surface. The success of this functionalization was evident from the appearance of a new vibration band in the FTIR spectra at  $1674\text{ cm}^{-1}$  corresponding to the formation of the amide bond (figure 2).<sup>DO WE ALSO HAVE ELEMENTAL ANALYSIS?</sup> The subsequent ATRPs were carried out under ARGET conditions to significantly reduce the amount of copper to parts per million (ppm) level. In this process the oxidatively stable  $\text{Cu}^{\text{(II)}}$  complexes are constantly transformed to active  $\text{Cu}^{\text{(I)}}$  species by a reducing agent, in our case tin(II) 2-ethylhexanoate.<sup>2627,28,29,30</sup> ARGET ATRP can tolerate a large excess of reducing agent and, as the result, can be conducted in the presence of limited amount of air.<sup>31</sup> The polymerizations were carried out with and without the addition of the sacrificial initiator ethyl 2-bromoisobutyrate (EBiB). Sacrificial initiators play an important role in the control of surface initiat-

ed ATRP by increasing the Cu(II) concentration, thus increasing the rate of deactivation process and thereby increasing the number of activation-deactivation cycles.<sup>32</sup> Moreover, it is a convenient indirect reporter for the molecular weight and polydispersity (PDI) of the surfaces grafted polymers provided there is a good correlation between the polymer growth from the surface and in solution.<sup>33,34,35,36,37</sup> In our case the sacrificial initiator EBiB is a  $\alpha$ -halogen ester whereas the surface initiator is an amide. The latter have been reported to be prone to a higher termination rate in the initial phase of conventional ATRP resulting in higher PDIs and molecular weights.<sup>38394041</sup> However, the aim of the present study is not to obtain truly monodisperse grafts but to accomplish a sufficiently good control over the polymerization so that a thick enough surface layers of polymer chains are formed with preserved polyHIPE morphology.

The grafting from polyHIPE surfaces was conducted by immersing an ATRP initiator-functionalized polyHIPE in the polymerization solution containing monomer, anisole, ligand, copper(II)bromide and tin(II) 2-ethylhexanoate as reducing agent, under nitrogen atmosphere. Initially the grafting of MMA was attempted in anisole (50/50 v/v) at 30°C using  $[MMA]/[EBiB]_{free}/[Cu^{II}]/[PMDETA]/[tin^{II}] = 747/1/0.1/1/1$  (PHIPE-g-PMMA1, Table 3). The excess ligand helps to maintain ?? the catalyst complex and protects it from destabilizing side reactions.<sup>REF</sup> The presence of excess reducing agent would increase the copper (I) : copper (II) ratio and enhance the polymerization rate.<sup>ref 21</sup> The same experimental conditions were applied without sacrificial EBiB initiator (PHIPE-g-PMMA2, Table 3). All thoroughly washed grafted substrates were characterized by ATR-FTIR spectroscopy and scanning electron microscopy (SEM). FTIR spectra of samples obtained with and without sacrificial initiator display characteristic PMMA signals such as the stretching vibrations of the ester carbonyl group at 1728  $cm^{-1}$  and the C-O stretching vibration between 1270 and 1000  $cm^{-1}$  (figure 2). Furthermore, SEM images suggest a relatively uniform grafting density within the observed area with preserved open cellular morphology (figure 3). Around 50 % (w/w) of PMMA grafted onto the polyHIPE was estimated from the difference of polyHIPE mass before and after MMA polymerization. These results

imply a successful PMMA grafting and good polymerization control in the homogeneous medium in the presence of the functional monolith.

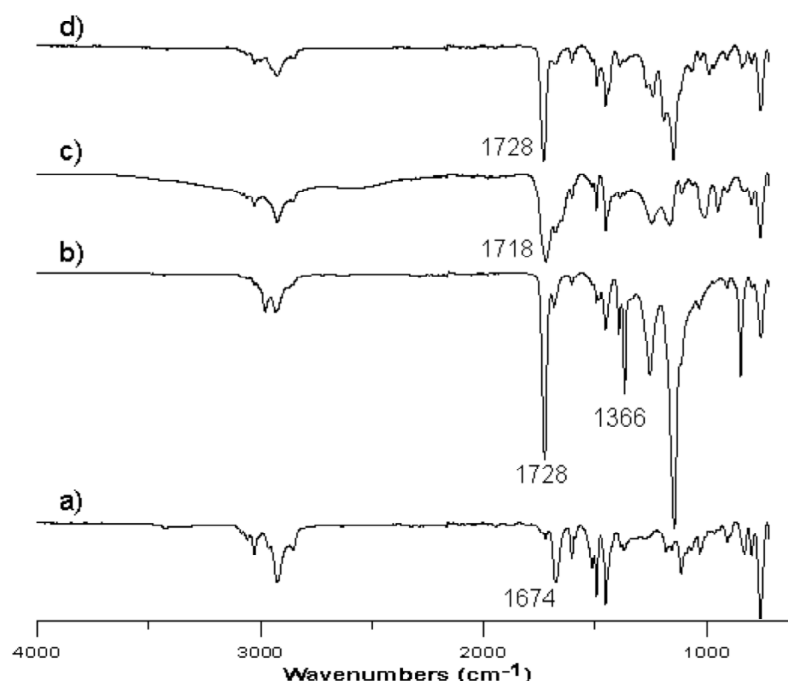


Figure 2. FTIR spectra from bottom to top of polyHIPE-Br, after *t*BA ARGET ATRP (PHIPE-*g*-PtBA5), after final PtBA deprotection with HCl (PHIPE-*g*-PAA5), and after MMA ARGET ATRP (PHIPE-*g*-PMMA2).

In order to introduce functional groups for bioconjugation on the surface of the monolith, the grafting of *tert*-butyl acrylate (*t*BA) via ARGET ATRP process from the ATRP initiator immobilized PHIPE surface was realized. Following removal of the *tert*butyl protecting group this would result in poly(acrylic acid) (PAA) functionalized polyHIPE. Dense PAA brushes are have successfully been used for protein separation using electrostatic interaction as well as for covalent binding of both positively and negatively charged biomolecules.<sup>42,4310(ref maty,langmuir2007)44 45</sup> The grafting of *t*BA from initiator-functionalized polyHIPE surfaces was realized in anisole (50/50 v/v) at 60°C using  $[EBiB]_{\text{free}}/[Cu^{II}]/[Ligand]/[tin^{II}] = 1/0.1/1/1$  targeting a theoretical degree of polymerization (DP) of 584 or 292, respectively. The same experimental conditions were applied without sacrificial initiator.

Two ligands, namely PMDETA and TPMA were tested since the rate constants of activation and deactivation can be dramatically altered through the choice of ligand. Complexes formed using TPMA (or Me<sub>6</sub>TREN) ligand have ATRP equilibrium constants several orders of magnitude higher than other ligands.<sup>46, 47</sup>

After intensive washing to remove all free PtBA chains, the samples were analyzed to confirm the success of the surface polymerization. Figure X shows a typical FTIR spectrum of a cut monolithic sample after *t*BA polymerization exhibiting characteristic PtBA bands such as the ester carbonyl at 1728 cm<sup>-1</sup> and methyl bending at 1367 cm<sup>-1</sup>.

Table 3:

Entry	Cu <sup>a)</sup> (ppm)	[M] [EBiB]	/ Tim e (h)	% Conv <sup>b)</sup>	Free polymer chains			PHIPE-g-Polymer  % weight ratio of grafted polymer
					Mn <sub>th</sub> <sup>c)</sup> (g/mol)	Mn <sup>d)</sup> (g/mol)	PDI <sup>d)</sup>	
PHIPE-g-PMMA1	96	-	6	-	-	-	-	55 <sup>e)</sup>
PHIPE-g-PMMA2	96	747	6	47	35 200	44 200	1.12	46 <sup>e)</sup>
PHIPE-g-PtBA1	61	-	8	-	-	-	-	7 <sup>d)</sup>
PHIPE-g-PtBA2	61	584	8	34	50 800	40 500	2.60	45 <sup>d)</sup>
PHIPE-g-PtBA3	61	-	16	-	-	-	-	29 <sup>d)</sup>

PHIPE-g-PtBA4	61	584	8	20	29 900	27 000	1.18	38 <sup>d)</sup>
PHIPE-g-PtBA5	61	584	15	34	50 800	49 000	1.20	70 <sup>d)</sup>
PHIPE-g-PtBA6	122	292	8	42	30 200	28 000	1.28	50 <sup>d)</sup>

a) Molar ratio vs. Monomer b) Conversion determined by <sup>1</sup>H NMR. c)  $M_{n_{th}}$  was calculated using the equation  $M_n = \text{conversion} \times [M]_0 \times [EBiB]_{free} \times M_{monomer}$ . d) Molar mass and experiment polydispersity determined by SEC using PMMA as standards. e) Estimated by the weight difference between the polyHIPE weight before and after polymerization. f) Calculated from TGA

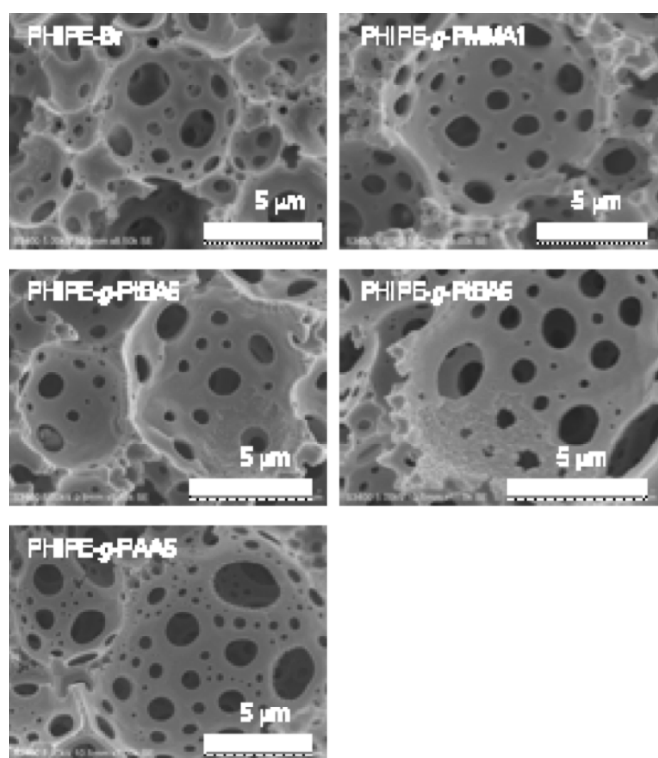


Figure 3. SEM images of functional polyHIPE samples.

The *tert*-butyl group of PtBA are known to undergo a thermal decomposition reaction at approximately 200°C to yield isobutylene and poly(acrylic acid) followed by a polymer decomposition above

400 °C.<sup>REF</sup> This particular chemistry provides a useful thermal handle for determining the amount PtBA polymer grafted onto the polyHIPE surface. Figure 4 shows the TGA result for X signifying two distinct decomposition stages. The first stage between 240-300°C is assigned to the weight loss of tert-butyl group, while the second stage between 400-500°C (the onset is 380°C) results from the weight loss of initial polyHIPE and residual PtBA segments. The weight fractions of PtBA in the polyHIPE sample based on the TGA results are summarized in Table 3. For the polymerization conducted without sacrificial initiator and PMDETA as a ligand only a low 7 weight % of grafting was achieved, while the polymerization conducted with TPMA yielded around 29 % PtBA grafting. Significantly better results were obtained when the polymerization was conducted with sacrificial initiator producing higher weight percentages of grafted polymer between 38 and 70 % depending on the experimental conditions (table 3). This confirms the clear benefits in the polymerization control in the presence of the sacrificial initiator. Information about the influence of the ARGET ATRP ligand was obtained from size exclusion chromatography (SEC) analysis of the free PtBA chains initiated by the sacrificial initiator. When PMDETA was used, broad polydispersity indices (PDI) of around 2.6 were measured which suggests a high rate of chain termination. On the other hand, throughout the polymerizations conducted with TPMA, SEC the traces of the free polymers were narrow ( $PDI < 1.3$ ) and symmetric, and shifted towards higher molar masses with increasing monomer conversion. This correlated very well with the increase in weight percentage of grafted polymer to the monolith surfaces (figure 4). While there is a difference in initiator structure between the sacrificial initiator and the surface initiators groups (ester vs. amide), the combined TGA and SEC results strongly imply very good control over grafting of tBA from the polyHIPE surface under these conditions. The so-obtained PtBA grafted polyHIPE substrates show a relatively uniform grafting density within the SEM imaged polyHIPE area (figure 3). Some images show small regions with surface inhomogeneities. These, however, do not necessarily indicate the absence of a polymer graft layer but are rather due to surface roughness. Moreover, the thickness of PtBA grafted on the surface by visual inspection appeared

higher when the molar masses of free PtBA chains increased. These observations underline the effectiveness of the grafting from via ARGET ATRP and confirm that the grafted PtBA with controllable molecular weight can be achieved by controlling the reaction time. Moreover, all materials were obtained a colourless monoliths in contrast to materials polymerized by conventional ATRP.

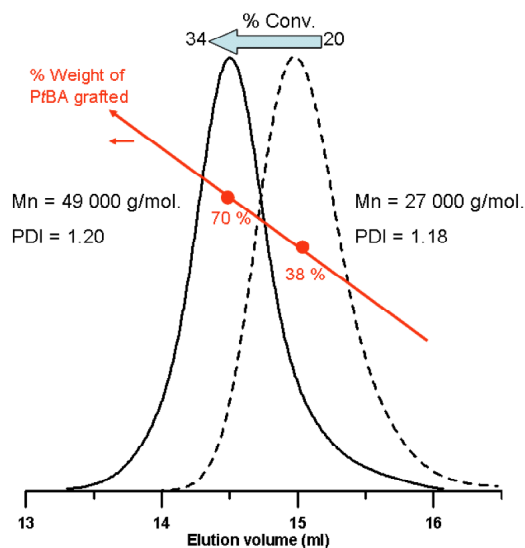


Figure 4. SEC traces of free PtBA chains obtained at 20 % (PtBA4) and 34 % (PtBA5) of conversion using the initial ratio  $[tBA]_0 / [EBiB]_{\text{free}} = 584$  and respectively the % weight of grafted PtBA grafted on the polyHIPE surface calculated by TGA analysis.

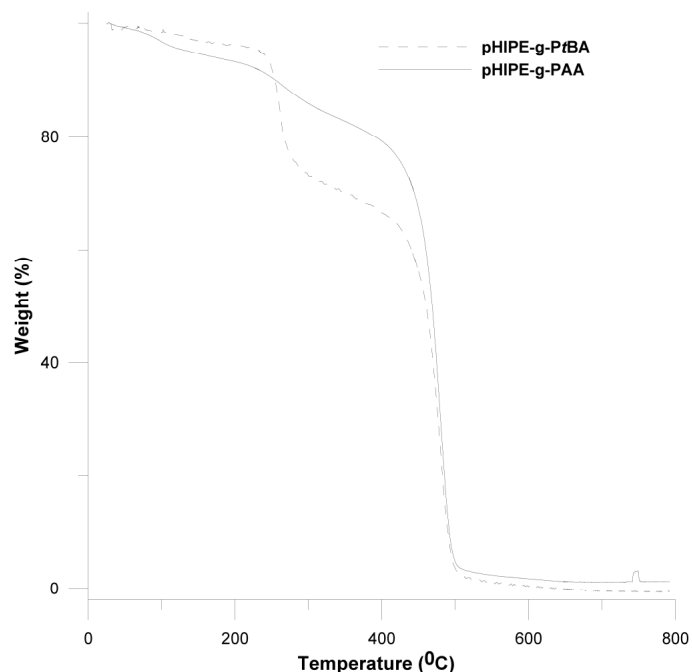


Figure 5. Thermogravimetric (TGA) curves of the PHIPE-g-PtBA2 and after PtBA deprotection (PHIPE-g-PAA2) under N<sub>2</sub>.

### *Surface property and conjugation*

The removal of the protecting groups from the grafted polymers was achieved by acidic hydrolysis with HCl. After deprotection the acid functionality on the surface of the substrate is clearly visible as a broad absorbance from 2800 to 3800 cm<sup>-1</sup> in the FTIR spectrum. Moreover, the carbonyl stretch slightly shifted from 1730 (ester) to 1718 (carboxylic acid) cm<sup>-1</sup> and the doublet band at 1366 cm<sup>-1</sup> corresponding to the stretching vibration of the *tert*-butyl methyl groups disappeared after hydrolysis. Further analysis by TGA permitted quantification of the successful deprotection. In all case, some residual decomposition between 240-300°C was detected associated with thermal removal of tBA groups. From this the estimated efficiency of the deprotection was calculated to be between 70 and 85 %. It is reasonable to assume that these unprotected groups are located close to the polyHIPE surface and are not easily accessible in the deprotection step. Nevertheless, following this protocol a highly



dense layer of PAA was homogeneously grafted on the polyHIPE surface, giving rise to changes in the macroscopic properties of the monoliths. All grafted polyHIPE samples (excepted PHIPE-g-PtBA1) display a clear change hydrophilicity after deprotection. As depicted in Figure 6, a drop of water easily penetrated a polyHIPE-g-PAA whereas polyHIPE-g-PtBA was completely hydrophobic preventing the water from entering the monolith. Most importantly, after deprotection the morphology of the polyHIPE was preserved and the cell and holes sizes appear more similar to those of the precursor monoliths due the significant mass loss ( $\sim 44\%$ ) associated with the deprotection (Figure 3).

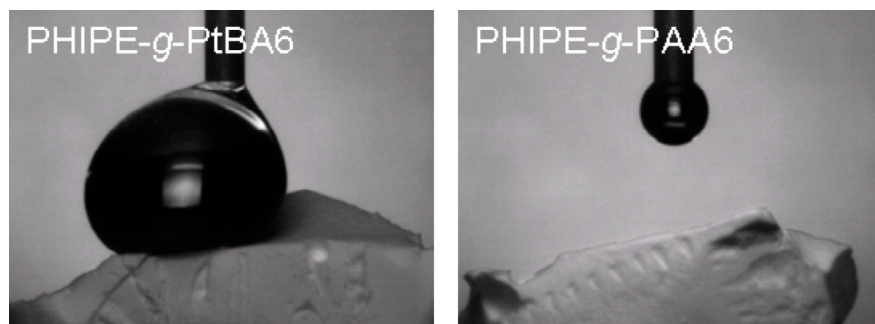


Figure 6. Change of hydrophilicity of polymer grafted polyHIPEs visualized by placing a drop of water on the monolith. In case no drop is visible immediate penetration of the water into the polyHIPE occurred.

Covalent bioconjugation to functional polyHIPEs was demonstrated in the past by covalent immobilization of proteins such as rAceGFP.<sup>48</sup> Recently, we reported the bioconjugation of eGFP and fluorescein isocyanate (FITC) to polypeptide grafted polyHIPE ( $-\text{COOH}$  or  $-\text{NH}_2$ )<sup>(our ref again)</sup> For comparison, eGFP was also selected to investigate the conjugation to polyHIPE-g-PAA6 as this protein can easily be visualized using commonly available filter sets designed for fluorescein and is among the brightest of the currently available fluorescent proteins.<sup>49</sup>

So, the coral-derived red fluorescent protein (DsRed) with its significantly red-shifted excitation and emission maxima (558 and 583 nm, respectively) has attracted tremendous interest because of its good complementation to the green fluorescent proteins and its enhanced mutants.<sup>50,51</sup> These features have rendered eGFP and DsRed two of the most popular probes and the best choice for most single-label fluorescent protein experiments.<sup>52,53</sup> The proteins immobilization were realized by the reaction of the  $\epsilon$ -amino groups of eGFP or DsRed lysine residues with the carboxyl groups of grafted PAA in buffer solution using common EDC/sulfo-NHS coupling chemistry (Table 2). The successes of the proteins immobilization were visualized by blue-light exposure pictures. The images in figure 7 clearly show that the eGFP and DsRed modified materials are highly fluorescent throughout the samples.

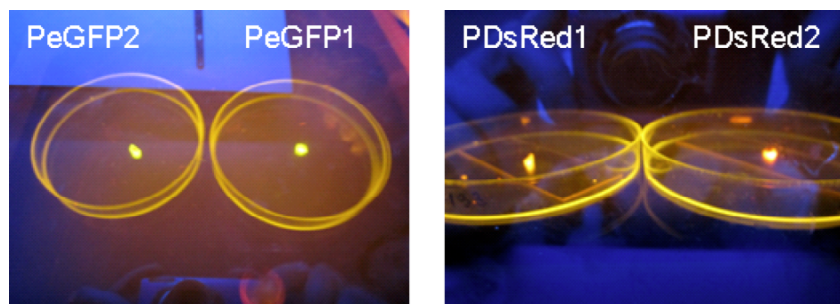


Figure 7. Pictures of functional polyHIPE-g-PAA after conjugation with eGFP (left) and DsRed (right) exposed to a blue light source.

Closer examination under a fluorescence optical microscope using a blue light filter also revealed intense green or red fluorescence in all PAA containing polyHIPEs conjugated with eGFP or DsRed (Figure 8). If no differences in the eGFP conjugation results were observed between the use of PBS or sodium carbonate buffer solution, for DsRed conjugation slightly higher fluorescence with the use of sodium carbonate buffer solution pH = 9.7 was observed.

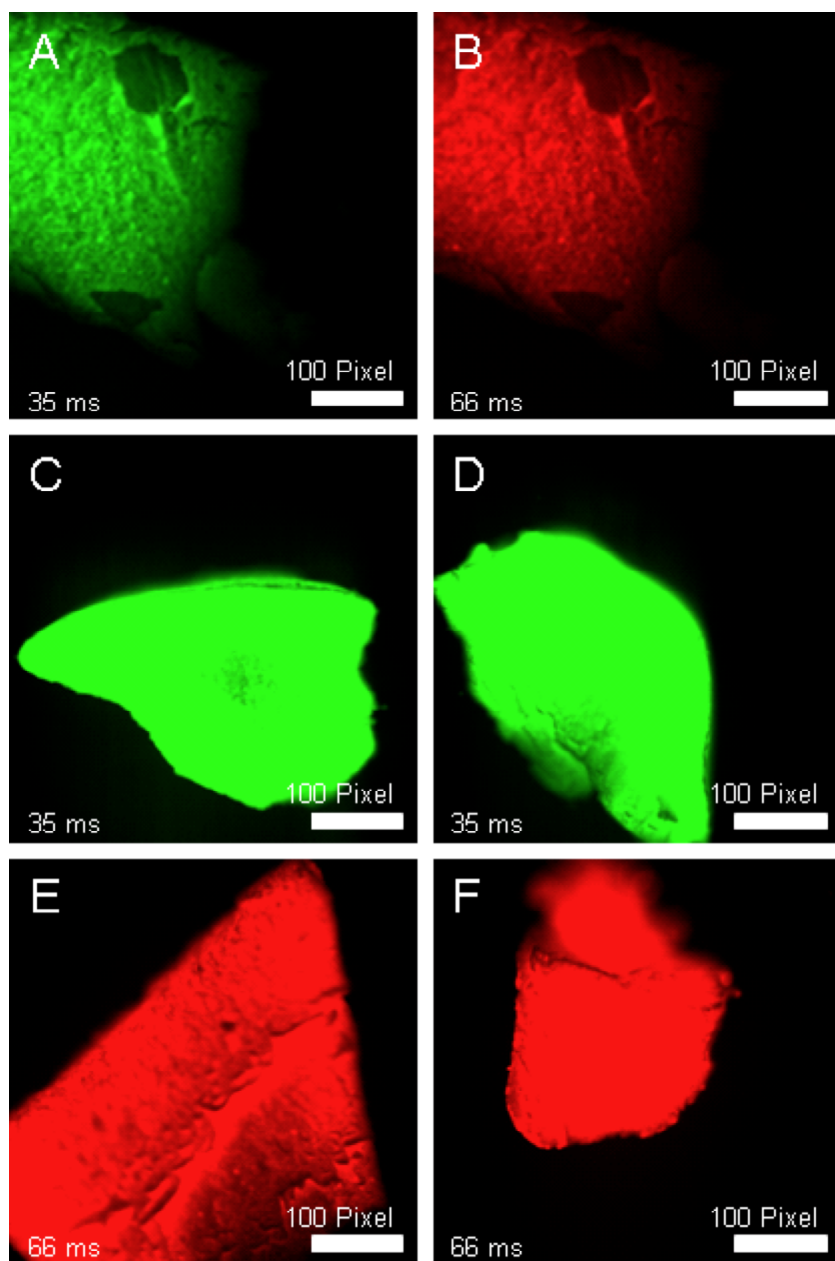


Figure 8. Fluorescence optical microscopy pictures at low exposure time (35 or 66 ms.) using a blue light filter. A) and B) control (polyHIPE-g-PAA6) C) sample PGFP1 D) sample PGFP2 E) sample PDsRed1 F) sample PDsRed2.

## Conclusions

eGFP and DsRed are two recombinant proteins that vary significantly in terms of their sequence, size and structure. Analysis of the amino acid sequence of both proteins shows that their sequences are only 23% identical. eGFP exists as a homodimer, with the two identical subunits having a molecular weight of 26.86 kDa each for a total molecular weight of 53.7 kDa (Yang et. al, 1996). DsRed exists as a homotetramer, with four identical subunits with a molecular weight of 25.93 kDa for a total molecular weight of 103.7 kDa (Yarbrough et. al, 2001). The proteins also differ in terms of their isoelectric point (pI). From the primary amino acid sequences of the proteins, the pI of eGFP is calculated to be 5.8 and the pI of DsRed is 7.8. The fact that the properties of eGFP and DsRed are dissimilar shows that this polyHIPE material is potentially amenable to the immobilization of numerous proteins upon its surface.

In this work, the capacity to conveniently convert the primary amine onto the polyHIPE-NH<sub>2</sub>, previously synthesized, to an atom transfer radical polymerization was realized to demonstrate the flexibility in monomer or method of polymerization introduced from the PHIPE-NH<sub>2</sub> precursor. The ATRP initiator group on the polyHIPE surface was successfully used to initiate ARGET ATRP of (meth)acrylic monomers, such as methyl methacrylate (MMA) or *tert*-butyl acrylate (*t*BA), which resulted in a dense coating of polymers on the polyHIPE surface. Homopolymers initiated by sacrificial initiator in the polymerization medium can be an indication of the grafted polymer brush length and permit an easy control of the amount of polymer grafted onto the monolith surface. Subsequent removal of the poly(*tert*-butyl acrylate) protecting groups yielded highly functional polyHIPE-g-poly(acrylic acid). The possibility to use the high density of function -COOH for secondary reaction was demonstrated by the successful conjugation of enhanced green fluorescent protein and coral derived red fluorescent protein, using EDC/sulfo-NHS chemistry, on the polymer 3D-scaffold surface. However, the materials and methodologies presented here open new potential in biosensor as well as in bioseparation applications from highly functional polyHIPEs.

Acknowledgments. F.A. would like to thank the European Commission for funding this work under the Marie-Curie Intra-European Fellowship program “Highly Functional Porous Materials for Bio-Diagnostic Sensors” (PoroSens, contract No. PIEF-GA-2009-252862). Financial support from the Science Foundation Ireland (SFI) Principle Investigator Award 07/IN1/B1792 (A.H.) is gratefully acknowledged. AH is a SFI Stokes Senior Lecturer (07/SK/B1241). **We thank Dr. P. Clarke and A. Harrington for provision of the DsRed vector.**

Supporting Information.

## References

- <sup>1</sup> Goddard, J. M.; Hotchkiss, J. H. *Prog. Polym. Sci.* **2007**, *32*, 698.
- <sup>2</sup> Grazu, J. M.; Abian, O.; Mateo, C.; Batista-Viera, F.; Fernandez-Lafuente, R.; Guisan, J. M. *Bio-technol. Bioeng.* **2005**, *90*, 597.
- <sup>3</sup> Wuang, S. C.; Neoh, K. G.; Kang, E. T.; Pack, D. W.; Leckband, D. E. *Adv. Funct. Mater.* **2006**, *16*, 1723.
- <sup>4</sup> Tugulu, S.; Arnold, A.; Sielaff, I.; Johnsson, K.; Klok, H. A. *Biomacromolecules* **2005**, *6*, 1602.
- <sup>5</sup> Kurosawa, S.; Aizawa, H.; Talib, Z. A.; Atthoff, B.; Hilborn, J. *Biosens. Bioelectron.* **2004**, *20*, 1165.
- <sup>6</sup> Xu, F. J.; Cai, Q. J.; Li, Y. L.; Kang, E. T.; Neoh, K. G. *Biomacromolecules* **2005**, *6*, 1012.
- <sup>7</sup> Huang, J.; Han, B.; Yue, W.; Yan, H. *J. Mater. Chem.* **2007**, *17*, 3812.
- <sup>8</sup> Xu, F. J.; Li, Y. L.; Kang, E. T.; Neoh, K. G. *Biomacromolecules* **2005**, *6*, 1759.
- <sup>9</sup> Xu, F. G.; Neoh, K. G.; Kang, E. T. *Prog. Polym. Sci.* **2009**, *34*, 719.
- <sup>10</sup> Barbey, R.; Lavanant, L.; Paripovic, D.; Schüwer, N.; Sugnaux, C.; Tugulu, S.; Klok, H.-A. *Chem. Rev.* **2009**, *109*, 5437.
- <sup>11</sup> Kimmins, S. D.; Cameron, N. R. *Adv. Funct. Mater.* **2011**, *21*, 211.
- <sup>12</sup> Barbetta, A.; Massimi, M.; Devirgiliis, L. C.; Dentini, M. *Biomacromolecules* **2006**, *7*, 3059.
- <sup>13</sup> Busby, W.; Cameron, N. R.; Jahoda, C. A. B. *Biomacromolecules* **2001**, *2*, 154.

- <sup>14</sup> Su, F.; Bray, C. L.; Tan, B.; Cooper, A. I. *Adv. Mater.* **2008**, *20*, 2663.
- <sup>15</sup> Moglia, R. S.; Holm, J. L.; Sears, N. A.; Wilson, C. J.; Harrisson, D. M.; Cosgriff-Hernandez, E. *Biomacromolecules* **2011**, *12*, 3621.
- <sup>16</sup> Barby, D.; Haq, Z. *European Patent 60 138*, March, 3, **1982**.
- <sup>17</sup> Cameron, N. R.; Sherrington, D. C. *Adv. Polym. Sci.* **1996**, *126*, 163.
- <sup>18</sup> Cameron, N. R.; Sherrington, D. C. *Macromolecules* **1997**, *30*, 5860.
- <sup>19</sup> Moine, L.; Deleuze, H.; Degueil, M.; Maillard, B. *J. Polym. Sci., Part A: Polym. Chem.* **2004**, *42*, 1216.
- <sup>20</sup> Cummins, D.; Wyman, P.; Duxbury, C. J.; Thies, J.; Koning, C. E.; Heise, A. *Chem. Mater.* **2007**, *19*, 5285.
- <sup>21</sup> Cummins, D.; Duxbury, C. J.; Quaedflieg, P. J. L. M.; Magusin, P. C. M. M.; Koning, C. E.; Heise, A. *Soft Matter* **2009**, *5*, 804.
- <sup>22</sup> Audouin, F.; Fox, M.; Larragy, R.; Huang, J. ; O'Connor, B. ; Heise, A. ref.
- <sup>23</sup> Jakubowski, W.; Min, K.; Matyjaszowski, K. *Macromolecules* **2006**, *39*, 39.
- <sup>24</sup> Matyjaszowski, K.; Jakubowski, W.; Min, K.; Tang, W.; Huang, J.; Braunecker, W. A.; Tsaversky, N. V. *Proc. Nat. Acad. Sci.* **2006**, *103*, 15309.
- <sup>25</sup> Audouin, F.; Knoop, R. J. I.; Huang, J.; Heise, A. *J. Polym. Sci., Part A: Polym. Chem.* **2010**, *48*, 4602.
- <sup>26</sup> Li, W.; Gao, H.; Matyjaszowski, K. *Macromolecules* **2009**, *42*, 927.
- <sup>27</sup> Jakubowski, W.; Matyjaszowski, K. *Angew. Chem.* **2006**, *118*, 4594.
- <sup>28</sup> Pietrasik, J.; Dong, H.; Matyjaszowski, K. *Macromolecules* **2006**, *39*, 6384.
- <sup>29</sup> Min, K.; Gao, H.; Matyjaszowski, K. *Macromolecules* **2007**, *40*, 2974.
- <sup>30</sup> Mueller, L.; Jakubowski, W.; Tang, W.; Matyjaszowski, K. *Macromolecules* **2007**, *40*, 6464.
- <sup>31</sup> Matyjaszowski, K.; Dong, H.; Jakubowski, W.; Pietrasik, J.; Kusumo, A. *Langmuir* **2007**, *23*, 4528.
- <sup>32</sup> Ejaz, M.; Yamamoto, S.; Ohno, K.; Tsujii, Y.; Fukada, T. *Macromolecules* **1998**, *31*, 5934.
- <sup>33</sup> Werne, T. V.; Patten, T. E. *J. Am. Chem. Soc.* **2001**, *123*, 7497.
- <sup>34</sup> Carlmark, A.; Malmstroem, E. *J. Am. Chem. Soc.* **2002**, *124*, 900.
- <sup>35</sup> Pyun, J.; Kowalewski, T.; Matyjaszowski, K. *Macromol. Rapid Commun.* **2003**, *24*, 1043.
- <sup>36</sup> Castelvetro, V.; Geppi, M.; Giaiacopi, S.; Mollica, G. *Biomacromolecules* **2007**, *8*, 498.
- <sup>37</sup> He, X. Y.; Yang, W.; Pei, X. W. *Macromolecules* **2008**, *41*, 4615.

- <sup>38</sup> Li, Y. T.; Tang, Y. Q.; Narain, R.; Lewis, A. L.; Armes, S. P. *Langmuir* 2005, 21, 9946– 9954.
- <sup>39</sup> Limer, A.; Haddleton, D. M. *Macromolecules* 2006, 39, 1353–1358.
- <sup>40</sup> Adams, D. J.; Young, I. J *Polym Sci: Polym Chem* 2008, 46, 6082–6090.
- <sup>41</sup> Gijs J.M. Habraken, Cor E. Koning, Andreas Heise, *Journal of Polymer Science: Part A: Polymer Chemistry*, Vol. 47, 6883–6893 (2009)
- <sup>42</sup> Cullen, S. P.; Liu, X; Mandel, I. C.; Himpsel, F. G.; Gopalan, P. *Langmuir* **2008**, 24, 913.
- <sup>43</sup> Ying, L.; Yin, C.; Zhou, R. X., Leong, K. W.; Mao, H. Q.; Kang, E. T. *Biomacromolecules* **2003**, 4, 157.
- <sup>44</sup> Kusumo, A.; Bombalski, L.; Lin, Q.; Matyjaszewski, K.; Scheinder, J. W., Tilton, R. D. *Langmuir* **2007**, 23, 4448.
- <sup>45</sup> Lei, Z.; Bi, S. *J. Biotechnol.* **2007**, 128, 112.
- <sup>46</sup> Tsarevsky, N. V.; Matyjaszewski, K. *Chem. Rev.* **2007**, 6, 2270.
- <sup>47</sup> Tang, W.; Matyjaszewski, K. *J. Am. Chem. Soc.* **2006**, 128, 1598.
- <sup>48</sup> Pierre, S. J.; Thies, J. C.; Dureault, A.; Cameron, N. R.; van Hest, J. C. M.; Carette, N.; Michon, T.; Weberskirch, R. *Adv. Mater.* **2006**, 18, 1822.
- <sup>49</sup> Heim, R.; Cubitt, A.; Tsien, R. *Nature* **1995**, 373, 663.
- <sup>50</sup> Matz, M. V.; Fradkov, A. F.; Labas, Y.A.; Savitsky, A. P.; Zaraisky, A. G., Markelov, M. L.; Lubyantsev, S.A. *Nat. Biotechnol.* **1999**, 17, 969.
- <sup>51</sup> Baird, G. S.; Zacharias, D. A.; Tsien, R. Y. *Proc. Natl. Acad. Sci. USA* **2000**, 97, 11984.
- <sup>52</sup> Cormack, B. P.; Valdivia, R.; Falkow, S. *Gene* **1996**, 173, 33.
- <sup>53</sup> Tsien, R. Y. *Ann. Rev. Biochem.* **1998**, 67, 509

Shimomura, O., Johnson, F. H. and Saiga, Y. 1962. Extraction, Purification and Properties of Aequorin, a Bioluminescent Protein from the Luminous Hydromedusan, *Aequorea*. *Journal of Cellular and Comparative Physiology* 59 (3), pp223-239.

Yang, F., Moss, L. G. and Phillips Jr, G. N. 1996. The molecular structure of green fluorescent protein. *Nat. Biotechnol.* 14 (10), pp1246-1251.

Yarbrough, D., Wachter, R. M., Kallio, K. 2001. Refined crystal structure of DsRed, a red fluorescent protein from coral, at 2.0-Å resolution. *Proceedings of the National Academy of Sciences* 98 (2), pp462-467.